

**FEDSM2008-55248**

## Self-assembly of Particles into 2D Lattices with Adaptable Spacing

N. Aubry  
 Department of Mechanical Engineering  
 Carnegie Mellon University  
 Pittsburgh, PA 15213  
 USA

S. Nudurupati, M. Janjua and P. Singh  
 New Jersey institute of Technology  
 Department of mechanical Engineering  
 Newark, New Jersey – 07102  
 USA

### ABSTRACT

It was recently shown in [1-3] that spherical particles floating on a fluid-fluid interface can be self-assembled, and the lattice between them can be controlled, using an electric field. The technique works for a broad range of fluids and particles, including electrically neutral (i.e., uncharged) particles and small particles (micro- and nano-sized particles). In this paper we show that the technique also works for rod-like and cubical particles floating on fluid-fluid interfaces. The method consists of sprinkling particles at a liquid interface and applying an electric field normal to the interface, thus resulting in a combination of hydrodynamic (capillary) and electrostatic forces acting on the particles. It is shown that the relative orientation of two rod-like particles can be controlled by applying an electric field normal to the interface. The lattice spacing of the self-assembled monolayer of rods can be increased by increasing the electric field strength. Furthermore, experiments show that there is a tendency for the rods to align so that they are parallel to each other. The alignment however is not complete. Similarly, the spacing between two cubes, as well as the spacing of a monolayer of cubes, can be adjusted by controlling the electric field strength.

### 1. Introduction

In recent years much effort has been directed to understand the behavior of particles trapped at fluid-fluid interfaces because of their importance in a wide range of applications, e.g., the self-assembly of particles at fluid-fluid interfaces resulting in novel nano structured materials, micro/nano manufacturing, the stabilization of emulsions, etc [4-10].

A popular mean used to assemble particles is based on the phenomenon of capillarity. A common example of capillarity driven self-assembly is the clustering of cereal flakes floating on the surface of milk. The floating cereal particles experience

attractive capillary forces due to the fact that when two such particles are close to each other, the deformed interface around them is not symmetric as the interface height between the particles is lowered due to the interfacial tension. This lowering of the interface between the particles gives rise to lateral forces that cause them to come together [10-13].

This technique, however, leads to uncontrollable clustering of particles, as capillary forces are attractive and increase with decreasing distance between particles. Capillarity induced clustering of (uncharged) particles has several deficiencies: (a) the resulting particle structure is usually not defect free: defects take place because particles physically block one another and the formed monolayer lacks long range order, (b) the lateral capillary forces become insignificant when the particle size is small (nanoparticle) (more precisely, when the dimensionless Bond number, which accounts for the particle and fluid densities, is much smaller than one), thus making particle assembly using this method restricted to the manipulation of mesoscale particles (larger than  $\sim 10 \mu\text{m}$ ) [13-16]; and (c) the lattice spacing is not adjustable.

We recently developed a technique which overcomes all of the above deficiencies by applying an external electric field normal to the interface causing particles trapped at the interface to experience an electrostatic force normal to the interface. This is a new phenomenon in which the electrostatic force arises because of the jump in the dielectric properties across the interface and varies as  $a^2$ , and not because the applied electric field is nonuniform, where  $a$  is the particle radius. (In a nonuniform electric field particles inside the suspending liquid experience an electrostatic force, called the dielectrophoretic force [17,18], which is weaker for small particles, as it varies as  $a^3$ ). The resulting self-assembly process is capable of controlling the lattice spacing statically or dynamically, forming virtually defect-free monolayers of monodispersed spherical particles, and manipulating a broad range of particle

sizes and types including nano-particles and electrically neutral particles. The electric field causes particles to experience electrostatic and capillary forces the magnitudes of which can be adjusted to control the lattice spacing of the formed monolayer. Since the strength of the electric field is easily varied with time, the formed microstructure can be changed in a dynamic fashion.

In this paper, we show that it is possible to align two rod-like particles, floating so that the cylinder generator is parallel to the interface, by applying an electric field. Also, the average distance between rods of a monolayer can be increased by applying an electric field. This is followed by similar results for cubic particles floating with the contact line pinned at their sharp edges.

## 2. Force balance for a particle trapped at the interface

The equilibrium position of a particle in the interface can be obtained by solving the governing equations for the two fluids and the momentum equation for the particle, which are coupled, along with the interface stress condition and a condition for the contact line motion on the particle surface. The problem of finding the particle's equilibrium position itself is formidable because the vertical capillary force at the line of contact of the three phases on the particle surface depends on the slope of the interface which in general requires the solution of the equations described above, and can be solved analytically only in simple situations [13,16]. The problem is even more challenging for a prismatic particle, since the capillary force depends on whether the meniscus attaches to the particle on a smooth face with a uniquely determined normal or at an edge where the normal is undefined, and so the contact line can become pinned, or both [16,19]. The stability of a given orientation of a particle is also an important issue, which can be different for small and large sized particles of geometrically similar shapes, as the gravity is important only for the latter.

Although particles used in this study are not spherical, for simplicity, we will describe results for spherical particles for which the closed form expressions for the forces and the lattice spacing can be obtained. Let us consider the vertical force balance equation for a spherical particle, when an electric field normal to the interface is present, which, in dimensionless form, can be written as [1,2]

$$2\pi \sin(\theta_c) \sin(\theta_c + \alpha) = -B f_b \left( \frac{\rho_a}{\rho_L}, \frac{\rho_p}{\rho_L}, \theta_c, \frac{h_2}{a} \right) + \quad (1)$$

$$W_E \left( \frac{\varepsilon_L}{\varepsilon_a} - 1 \right) f_v \left( \frac{\varepsilon_a}{\varepsilon_L}, \frac{\varepsilon_p}{\varepsilon_L}, \theta_c, \frac{h_2}{a} \right)$$

Here  $B = \rho_L a^2 g / \gamma$  is the Bond number,  $W_E = \varepsilon_0 \varepsilon_a \frac{a E^2}{\gamma}$  is

the electric Weber number and  $f_b, f_v$  are dimensionless buoyancy and vertical electric force coefficients, which are

$O(1)$ , but have to be determined. Also,  $E$  is the applied electric field strength (or the RMS value of the electric field in an AC field),  $\varepsilon_p, \varepsilon_a$  and  $\varepsilon_L$  are the dielectric constants of the particle, the upper fluid and the lower fluid, respectively,  $\varepsilon_0$  is the permittivity of free space, and  $\theta_c$  and  $h_2$  being defined in figure 1. The force due to the contact line tension and the particle charge, if present, can also be included in the above equation.

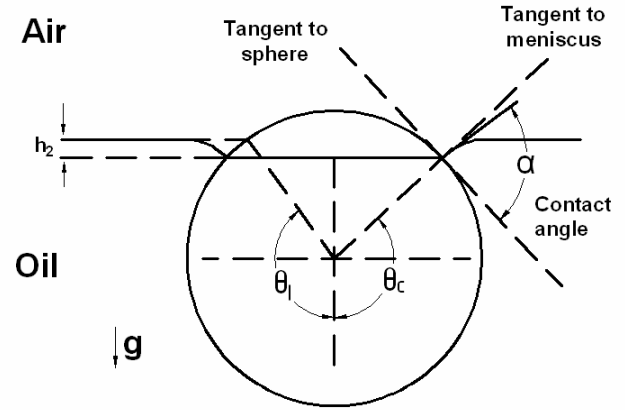


Figure 1. Schematic of a heavier than liquid hydrophilic (wetting) sphere of radius  $a$  hanging on the contact line at  $\theta_c$ . The point of extension of the flat meniscus on the sphere determines the angle  $\theta_1$  and  $h_2$ . The angle  $\alpha$  is fixed by the Young-Dupré law and  $\theta_c$  by the force balance.

Clearly, as the particle radius  $a$  approaches zero, the Bond number  $B = \rho_L a^2 g / \gamma \rightarrow 0$ . In this limit, in the absence of an electrostatic force, the right hand side of equation (1) is zero and thus  $\sin(\alpha + \theta_c) \approx 0$  or  $\theta_c \approx \pi/2 - \alpha$  (see figure 1). This means that a small particle floats so that the interfacial deformation is negligible. It can be shown that the lateral capillary force which arises from the interfacial deformation, in this limit, is also negligible compared to the random thermal forces. For particles floating on water, this limit is reached when the particles radius is approximately  $10 \mu\text{m}$  (see [13,16]). Therefore, groups of small spherical and disk shaped particles cannot cluster by this mechanism. After reaching their respective equilibrium positions in the interface, they no longer substantially deform the interface. Small particles, however, can interact by other mechanisms some of which are described below [19]. Furthermore, when particles are partially immersed in a thin liquid film and their weight is supported by the substrate below, the arguments just given are not applicable and the interface deformation can be significant even for small particles [13].

Another important limiting case is that for which the Bond number approaches zero, but the electric Weber number does not. This situation arises, for instance, for small particles when the magnitude of the electric field is sufficiently large. The equilibrium position of a particle within the interface in this

case is determined by the balance of the interfacial and electrostatic forces. The interface can then be deformed by the particle, in which case, as discussed below, the lateral (electric field induced) capillary forces are present and can cause nano sized particles within the interface to cluster [1,2].

## 2.1 Vertical electrostatic force

It is well-known that while an isolated uncharged particle placed in a uniform electric field becomes polarized, it does not experience any electrostatic force. This, however, is not the case for a particle floating at a fluid-fluid interface because of the mismatch between the dielectric constants of the two fluids involved (see figure 2), and thus the electric field around a particle is not symmetric about the fluid-fluid interface [1,2]. Moreover, from symmetry it is clear that the electrostatic force acting on an isolated spherical particle at an interface can only be in the direction normal to the interface, but depending on the parameter values it can be either upward or downward. If the particle is charged, a coulomb force also acts on the particle. In addition, when there are other particles present at the interface they interact with each other via dipole-dipole interactions [20-25].

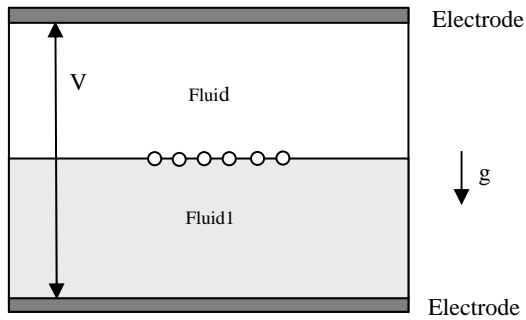


Figure 2. Schematic of the experimental setup used to control assembly of particles on a fluid-fluid interface. The distance between neighboring particles is controlled by adjusting the applied voltage.

We performed numerical simulations to show that the vertical component of the electrostatic force in a DC field (or time averaged force in an AC field) acting on a particle can be written as [2,3]:

$$F_{ev} = a^2 \varepsilon_0 \varepsilon_a \left( \frac{\varepsilon_L}{\varepsilon_a} - 1 \right) E^2 f_v \left( \frac{\varepsilon_L}{\varepsilon_a}, \frac{\varepsilon_p}{\varepsilon_a}, \theta_c, \frac{h_2}{a} \right). \quad (2)$$

Here  $f_v \left( \frac{\varepsilon_L}{\varepsilon_a}, \frac{\varepsilon_p}{\varepsilon_a}, \theta_c, \frac{h_2}{a} \right)$  is a dimensionless function of the included arguments ( $\theta_c$  and  $h_2$  being defined in figure 4). The

factor  $\left( \frac{\varepsilon_L}{\varepsilon_a} - 1 \right)$  ensures the fact that the force is zero when

$\frac{\varepsilon_L}{\varepsilon_a} = 1$  as the fluids dielectric constants are the same in this

case (as noted above, the electrostatic force acting on a particle in a bulk fluid subjected to a uniform electric field is zero). Notice that the dependence of the electrostatic force on the particle radius  $a$  is quadratic compared to the cubic dependence of the dielectrophoretic (DEP) force which acts on a particle in a non-uniform electric field [17,18], and therefore the origin of the former is different from that of the DEP force experienced by a particle inside the suspending liquid. The influence of electrowetting can be included in this analysis by modifying the effective contact angle [26]. Notice that a change in the contact angle (due to electrowetting) will cause a particle to move normal to the interface to satisfy the new contact angle requirement. However, assuming that the only change is in the contact angle, it will not cause the interface to deform (because if the interface around the particle is deformed, the particle will experience a vertical capillary force which will remain unbalanced since the particle does not experience an additional external vertical force.).

## 2.2 Lateral forces between particles

The deformation of the interface due to the trapped particles gives rise to lateral capillary forces which cause them to cluster (see figure 1) [11,13]. The attractive capillary forces arise due to the fact that when two floating particles are close to each other the interface height between the particles is lowered due to the interfacial tension. This lowering of the interface between the particles gives rise to lateral forces that cause them to come together. The floating behavior of small (micro and nano) sized particles and prismatic particles is even more complex because the attractive force does not arise because of the particle's buoyant weight, but by other more complex mechanisms.

As noted earlier, our recent experiments show that an externally applied electric field can be used to control the self-assembly process of particles at a fluid-fluid interface, and that the distance between particles can be varied by changing the strength of electric field [1,2]. This is a unique approach which allows the spacing between particles to be controlled dynamically. Also, when the electric field intensity is of  $O(10^6)$  volts/m the electric force is sufficient for manipulating submicron to nano sized particles as the associated energy is greater than  $kT$ . This is possible because the electrostatic force normal to the interface, which is balanced by the vertical capillary force, causes the interface to deform. The electrostatic force thus plays a role similar to that of the particle's buoyant weight in causing lateral capillary forces. In addition, in the presence of an electric field (uncharged) particles become polarized and experience repulsive forces arising because of the dipole-dipole interactions [20,25].

We numerically computed the electrostatic repulsive force arising due to the dipole-dipole interaction accounting for the

fact that the fluid's dielectric constant jumps across the interface and found that it can be written as [1,2]

$$F_D(r) = \varepsilon_0 \varepsilon_a \left( \frac{\varepsilon_L}{\varepsilon_a} + 1 \right) a^2 E^2 \left( \frac{a}{r} \right)^4 f_D \left( \frac{\varepsilon_L}{\varepsilon_a}, \frac{\varepsilon_p}{\varepsilon_a}, \theta_c, \frac{h_2}{a} \right) \quad (3)$$

where  $f_D$  is a dimensionless function of the included arguments, with the force depending upon the sixth power of  $a$  and on the fourth power of the inverse of the distance  $r$  between the particles. The repulsive interaction force was shown to be stronger than the random Brownian force indicating that the externally applied electric field can be used to manipulate nanoparticles within a fluid-fluid interface.

We conducted an analysis to determine the capillary forces between two particles in which the dynamical effects were not considered [1,2]. Analysis further assumed the interfacial deformation to be small, the electric force on the particles was estimated numerically by assuming that the interface was not deformed, and the electric force on the fluid interface and the resulting deformation were neglected. Based on this analysis, we concluded that in the presence of an electric field, particles experience repulsive electrostatic forces which are short ranged (vary as  $r^{-4}$ ), and attractive capillary forces which are long ranged (vary as  $r^{-1}$ ). The dimensionless equilibrium separation  $r_{eq}/(2a)$  between two particles, obtained by equating the repulsive electrostatic force and the lateral capillary force is

$$\frac{r_{eq}}{2a} = \frac{1}{2} \left[ \frac{2\pi\varepsilon_0\varepsilon_a \left( \frac{\varepsilon_L}{\varepsilon_a} + 1 \right) \gamma E^2 f_D}{a \left( -\varepsilon_0\varepsilon_a \left( \frac{\varepsilon_L}{\varepsilon_a} - 1 \right) E^2 f_v + \frac{4}{3} \pi a \rho_p g f_b \right)^2} \right]^{\frac{1}{3}} \quad (4)$$

The dimensionless parameters  $f_v$ ,  $f_D$  and  $f_b$  themselves depend on several parameters, and have to be obtained numerically or from the experimental data.

### 2.3 Non-spherical particles

As noted above, if the buoyant weight of a spherical particle is not negligible, the vertical capillary force, which arises because of the deformation of the interface, is needed to keep it floating. The deformed interface around an isolated spherical particle is symmetric about the vertical passing through its center, and thus the lateral capillary force that arises due to this deformation is independent of the radial direction. The deformed interface around prismatic and non spherical particles, however, is not symmetric, and consequently their clustering behavior is more complex.

In general, for non-spherical and prismatic particles deformed interface is such that the interface slope at the contact line on the particle's surface varies, as the direction of the

normal to the surface varies. In fact, on a part of the contact line the slope of the interface can be in the upward direction, and for the remaining part it can be in the downward direction. Notice that the slope of the interface determines the direction of the capillary force which acts on the particle. Thus, the magnitude of the vertical component of capillary force varies along the contact line, and its direction on a portion of the contact can be in the downward direction. As a result, although the total vertical capillary force is still equal to the buoyant weight, the contribution of some sections of the contact line to the vertical capillary force can be negative and for some positive.

The above implies that two particles can attract or repel depending on the interface deformation between them, i.e., if both particles cause upward or downward interface deformation of the interface, they attract; otherwise they repel. Depending on the form of the asymmetric deformation around them, such particles can assemble into several different periodic arrangements, e.g., hexagonal or cubic.

Also note that a small particle, with negligible buoyant weight, can cause an asymmetric deformation of the interface if the contact line undulates on its surface [19]. These undulations in the contact line can arise because of the surface roughness, caused by edges and irregular shape, chemical inhomogeneities, and Brownian motion. At present, analysis similar to that presented in the previous subsection for spherical particles, is not available for non-spherical particles.

## 3. Results

We next present experimental results describing the clustering behavior of rod-like and cubic particles floating on the surface of corn oil. Experiments were conducted in a device for which the distance between the electrodes is 8 mm and the diameter of the circular cross-section is 48 mm (see figure 2).

### 3.1 Rod-like particles

In our experiments the rod-like particles float with their generator parallel to the interface. In this configuration, the interfacial deformation varies along the contact line. In fact, the interfacial deformation at the contact line on the curved surfaces can be quite different from the deformation at the flat ends. Notice that although the contact-angle condition is satisfied at both the curved and flat surfaces, the direction of the normal at the two surfaces can be quite different, and as a result, the interfacial deformation at these surfaces can also be different. Consequently, the lateral attraction due to capillarity is not the same along all radial directions.

In the absence of an externally applied electric field rods cluster, but since the interfacial deformation caused by particles is asymmetric, they arrange in certain preferred orientations that depend on their initial positions as well as orientations. In the presence of an externally applied electric field, when the

electric field magnitude is sufficiently large, rods become aligned and are approximately parallel to each other.

We next present results for two rods floating on the surface of corn oil. The diameter of the rods is  $39.8\ \mu\text{m}$ , and the length of one rod is  $255.2\ \mu\text{m}$  and of the second  $260\ \mu\text{m}$ . Two different initial orientations of the rods are considered. We first consider the cases for which the electric field is not present.

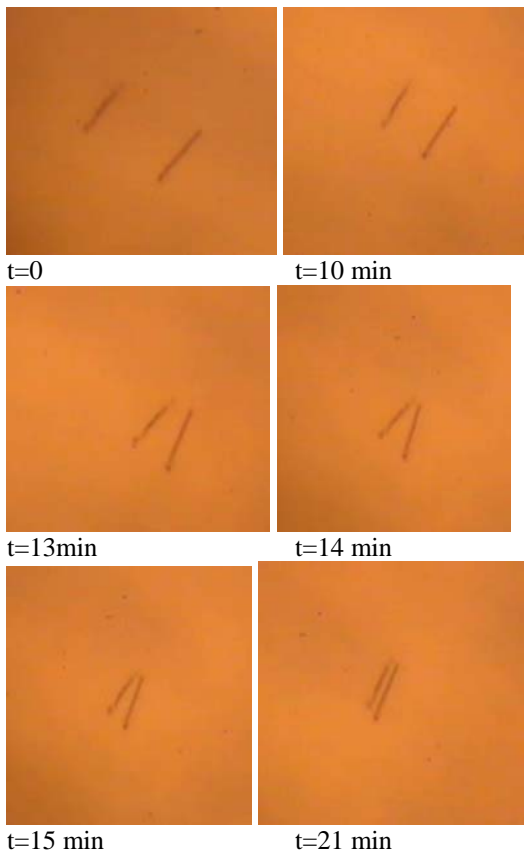


Figure 3. The transient positions of two rods showing attraction between them. The electric field is not present. The rods diameter is  $39.8\ \mu\text{m}$  and the length of the left rod is  $255.2\ \mu\text{m}$  and the right rod is  $260\ \mu\text{m}$ . Initially, the rods are approximately parallel. But, when they come closer, they rotate such that the upper ends come in contact earlier. After coming in contact, the rods become approximately parallel.

Figure 3 shows the case in which the two rods are initially approximately parallel to each other and the line joining their centers is perpendicular to the rods. The rods maintain this approximate orientation as they come closer. But when the distance between them is smaller, they begin to turn so that the upper ends of the rods are closer. This becomes more clear in the photograph taken at  $t=13\ \text{min}$ . The rods continue to come closer and rotate, and the rate of approach increases with decreasing distance between them. The upper ends touch at

$t=14\ \text{min}$ . The lower ends continue to come closer and touch at  $t=21\ \text{min}$ . In this final configuration the rods are again parallel to each other, but the upper ends of the rods are closer than the lower ends. This is probably due to the fact that the end planes for one of the rods, or both, are not completely normal to the rod's axis. This asymmetry makes the interfacial deformation caused by the upper ends of the rod to be such that the attractive capillary force between them is larger than between the lower ends.



Figure 4. Attraction between two floating rod. The parameters are the same as in Figure 3. Initially, the rods are approximately parallel with their flat ends facing each other. As the rods come closer, they align so that they are approximately parallel to the line joining their centers. They maintain this orientation until touching, but after touching they rotate and are no longer parallel.

We next consider the case for which the initial positions and orientations of the two rods are such that they are approximately parallel to the line joining their centers (see Figure 4). The rods come closer under the action of the attractive capillary force while approximately maintain their initial orientations. The approach velocity increases with decreasing distance between the rods. Notice that the rods are approximately parallel when they come in contact at  $t=270\ \text{s}$ , but afterwards they rotate slightly and are no longer parallel (see Figure 4 at  $t=20\ \text{min}$ ). This occurred because the end surfaces of the two rods were not completely perpendicular to the rods' axes.

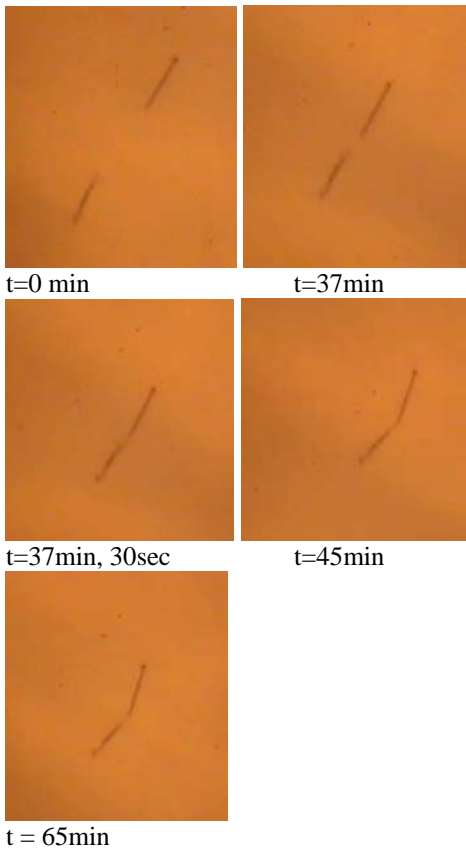


Figure 5. Attraction between two floating rod in the presence on an externally applied electric field. The voltage applied is 5000 V. The other parameters are the same as in Figure 4. As the rods come closer, they align so that they are approximately parallel to the line joining their centers. They maintain this orientation until touching, but, as in Figure 4, after touching they rotate and form an angle. The approach velocity is reduced by the electric field.

In Figure 5 we consider the initial configuration of Figure 4, but in the presence of an electric field normal to the interface. The two rods still attract because of the attractive capillary force, and come closer with increasing time and touch at  $t=37$  min 30s. They approximately maintain their initial orientations, i.e., remain oriented along the line joining their centers. Furthermore, after touching they rotate and are no longer parallel to each other. The only influence of the electric field is on the approach velocity which is smaller in the presence of the electric field.

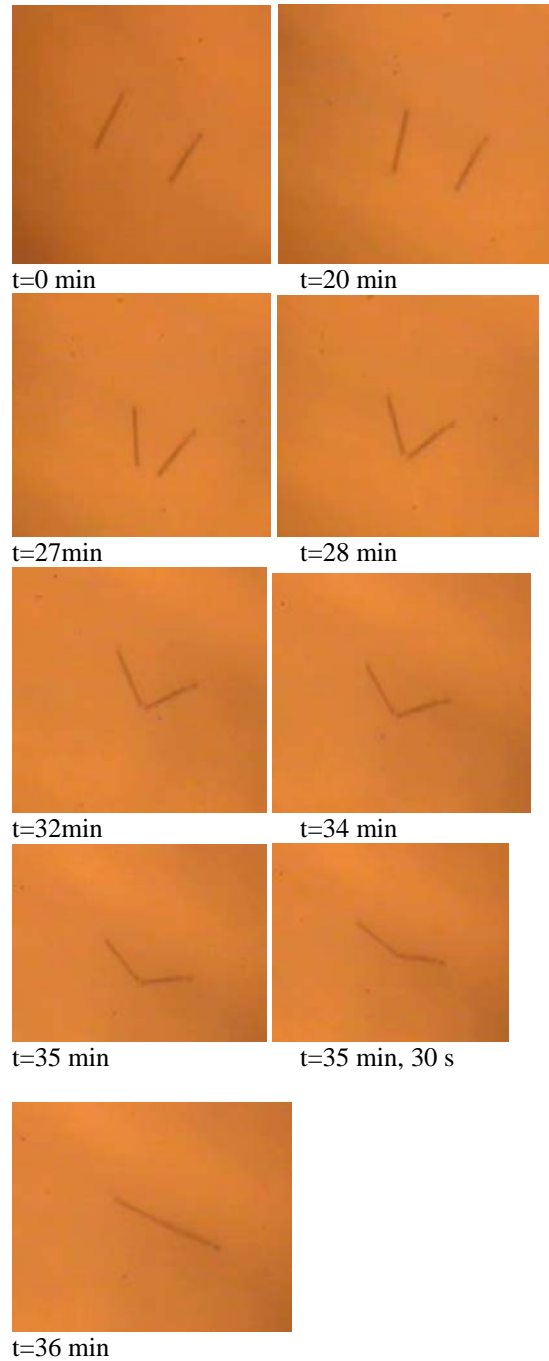
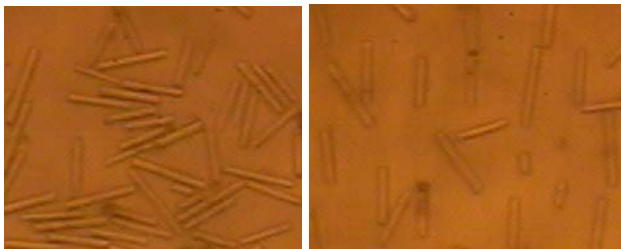


Figure 6. Attraction between two floating rods in the presence on an externally applied electric field. The voltage applied is 5000 V. The other parameters are the same as in Figure 3. In the beginning, the rods are approximately parallel, but when they are closer, they rotate so that the lower ends first come in contact. After coming in contact, the rods rotate so that the angle between them increases with time. In the final configuration, the rods are aligned parallel to the line joining their centers.

In Figure 6 we consider the influence of electric field on the attraction of rods when their positions are such that the rods are approximately perpendicular to the line joining their centers. As was the case in Figure 3, the rods come closer with increasing time and when they are away from each other they remain parallel. The approach velocity is smaller than for the case when the electric field is not present. This shows that the electric force between the rods is repulsive. However, as before, when the distance between is smaller than a critical values they rotate and the lower end of the two rods come in contact. Once this happens, the rods begin to rotate so the angle between them increases to 180 degrees. This is the opposite of the case shown in Figure 3, without the electric field, where the angle decreased. This shows that the influence of the electric field is to rotate the rods so that they align to form a line with their ends touching.



(a) 0 volts, (b) 5000 volts

Figure 7. The figure shows that rods floating on the surface of corn oil cluster. When a voltage of 5000 V is applied, the distance between rods increases and they align approximately parallel to each other.

In Figure 7 we consider the case in which many rods are sprinkled on the corn oil surface. The figure shows that in the absence of the electric field rods cluster but there is no overall pattern. This is consequence of the fact that when the distance between the rods is of the same order as the rod size they physically block each other, preventing them from organizing in a pattern. The distance between rods increases when a voltage of 5000 V is applied. The resulting electric also causes the rods to align parallel to each other. The figure also shows that there is tendency to form lines with the tips of the rods touching. However, the alignment is not complete because of the presence of the neighboring rods and relatively large variation in their length.

### 3.2 Cubic particles

Figure 8 shows that a cubical particle floats such that the contact line is pinned at its top sharp edges. The floating behavior of prismatic particles is therefore different from that of a spherical particle because the contact line is pinned at the sharp edges [16], and can remain pinned even when an electric

field normal to the interface is applied. This is shown in Figure 8 for the case of two cubes which cluster under the action of capillary forces when the electric field is not applied. After the electric field of sufficiently large magnitude is applied, the cubes separate and the distance between them increases with increasing electric field strength (see Figure 9). Also, since the interfacial deformation caused by a cube is asymmetric, they arrange in certain preferred orientations.

Figure 10 shows that in the absence of an externally applied electric field cubes cluster, but when an electric field of sufficiently large magnitude is applied the cluster is broken. The figure also shows that spacing of the monolayer can be controlled by changing the electric field strength. Since the contact line remains pinned at the sharp edge, the electrowetting effect is not present [26] (the contact angle, however, can change because the vertical electrostatic force on the particle [1,2].).



(a) 0 volts, (b) 2000 volts, (c) 4000 volts

Figure 8. The floating behavior of two cubes (size ~ 150 μm) is shown. The lattice distance between the cubes increases with electric field strength. The contact line is pinned at the upper edge of the cubes, and remains pinned even when the electric field is present.

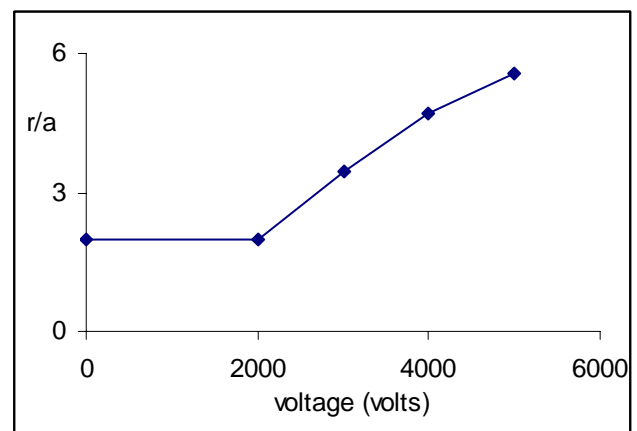
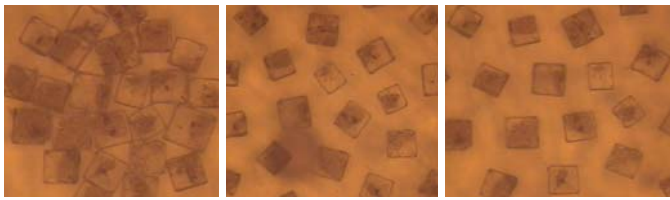


Figure 9. The dimensionless distance between two cubes is plotted as a function of the applied voltage. Notice that there a critical voltage at which the two cubes separate.



(a) 0 volts, (b) 3000 volts, (c) 5000 volts

Figure 10. An assembled monolayer of cubes. In the absence of the electric field cubes cluster. When an electric field normal to the interface is applied the lattice spacing increases with increasing electric field strength. The contact line is pinned at the upper edge of the cubes, and remains pinned even when the electric field is present.

#### 4. Conclusions

Experiments performed using rod-like and cubic particles show that the distance between them and their relative orientations can be controlled by applying an electric field normal to the interface. The electric field causes particles on the fluid/fluid interface to experience an electrostatic force normal to the interface. In addition, particles become polarized and interact with each other via dipole-dipole interactions, which for the particles trapped on the interface is repulsive. The distance between the particles is determined by the balance of the attractive capillary forces and the repulsive dipole-dipole forces. In the presence of the electric field, the preferred orientation for rod-like particles is to align parallel to each other, and form lines with their ends touching.

#### 5. References

- Aubry, N., P. Singh, M. Janjua and S. Nudurupati, Assembly of defect-free particle monolayers with dynamically adjustable lattice spacing, *Proceedings of the National Academy of Sciences*, 105, 10.1073/pnas.0712392105 (2008).
- Aubry, N. and P. Singh, Physics underlying the controlled self-assembly of micro and nanoparticles at a two-fluid interface using an electric field, submitted to *Physical Rev. E* (2007).
- Aubry N, Singh P (2007) Electrostatic forces on particles floating within the interface between two immiscible fluids, Paper IMECE2007-44095, Proceedings of 2007 ASME International Mechanical Engineering Congress and Exhibition, Nov. 11-15 Seattle, WA.
- Murray CB, Kagan CR, Bawendi MG (2000) Synthesis and characterization of monodisperse nanocrystals and close-packed nanocrystal assemblies. *Annu. Rev. Mater. Sci.* 30: 545-610.
- Tan Z, Zhang, Wang Y, Glotzer SC, Kotov NA (2006) Self-Assembly of CdTe Nanocrystals into Free-Floating Sheets, *Science* 314: 274-278.
- Bowden N, Choi IS, Grzybowski BA, Whitesides GM (1999) Mesoscale self-assembly of hexagonal plates using lateral capillary forces: synthesis using the "capillary bond", *J. Am. Chem. Soc.* 121: 5373-5391.
- Bowden NA, Terfort A, Carbeck J, Whitesides GM (1997) Self-assembly of mesoscale objects into ordered two-dimensional arrays, *Science* 276: 233-235.
- Grzybowski BA, Bowden N, Arias F, Yang H, Whitesides GM (2001) Modeling of menisci and capillary forces from the millimeter to the micrometer size range, *J. Phys. Chem. B* 105: 404-412
- Wasielowski MR (1992) Photoinduced electron transfer in supramolecular systems for artificial photosynthesis, *Chem. Rev.* 92: 435.
- Balzani V, Venturi M, Credi A (2003) Molecular devices and Machines, Wiley VCH, Weinheim.
- Chan DYC, Henry JD, Jr. White LR (1981) The interaction of colloidal particles collected at the fluid interface, *J. Colloid Interface Sci.* 79: 410.
- Fortes MA (1982) Attraction and repulsion of floating particles, *Can. J. Chem.* 60: 2889.
- Kralchevsky PA, Nagayama K (2000) Capillary interactions between particles bound to interfaces, liquid films and biomembranes, *Advances in Colloid and Interface Science* 85: 145-192.
- Lucassen J (1992) Capillary forces between solid particles in fluid interfaces. *Colloids Surf.* 65: 131-137.
- Nicolson MM (1949) The interaction between floating particles, *Proc. Cambridge Philosophical Soc.* 45: 288.
- Singh P and Joseph DD (2005) Fluid dynamics of Floating particles, *J. Fluid Mech.* 530: 31-80.
- Pohl HA (1978) Dielectrophoresis, Cambridge: Cambridge University Press.
- Jones TB (1995) Electromechanics of particles, Cambridge University Press.
- Stamou D, Duschl C (2000) Long-range attraction between colloidal spheres at the air-water interface: The consequence of an irregular meniscus. *Physical Rev. E* 62: 5263-5272.
- Klingenberg DJ, Van Swol S, Zukoski CF (1989) Simulation of electrorheological suspensions, *J. Chem. Phys.* 91: 7888-7895.
- Kadaksham J, Singh P, Aubry N (2004), Dynamics of pressure driven flows of electrorheological suspensions subjected to spatially non-uniform electric fields, *J. Fluids Eng.* 126: 170-179.
- Kadaksham J, Singh P and Aubry N (2004) Dielectrophoresis of nano particles, *Electrophoresis* 25: 3625-3632.



23. Kadaksham J, Singh P and Aubry N (2005) Dielectrophoresis induced clustering regimes of viable yeast cells, *Electrophoresis*, 26, 3738–3744.
24. Kadaksham J, Singh P, Aubry N (2006) Manipulation of Particles Using Dielectrophoresis, *Mechanics Research Communications* 33: 108-122.
25. Aubry N, Singh P (2006) Control of Electrostatic Particle-Particle Interactions in Dielectrophoresis, *Euro Phys. Lett.* 74: 623–629.
26. Mugele F, Baret J (2005) Electrowetting: from basics to applications, *J. Phys.: Condens. Matter* 17: R705–R774.